

Lion swarm optimization for grid connected PV system with improved SEPIC

P. Annapandi¹, D. Lakshmi², B. Kavya Santhoshi³, P. Annapoorani⁴

¹Department of Electrical and Electronics Engineering, Francis Xavier Engineering College, Tirunelveli, India

²Department of Electrical and Electronics Engineering, AMET Deemed to be University, Chennai, India

³Department of Electrical and Electronics Engineering, Godavari Institute of Engineering and Technology (Autonomous), Rajamahendravaram, India

⁴Department of Electrical and Electronics Engineering, Vel Tech Multi Tech Dr. Rangarajan Dr. Sakunthala Engineering College, Avadi, India

Article Info

Article history:

Received Jul 11, 2023

Revised Feb 22, 2024

Accepted Mar 13, 2024

Keywords:

1 ϕ VSI

Improved SEPIC

LSO

PI controller

PV system

ABSTRACT

The wide deployment of grid-connected renewable energy system has piqued immense attention recently, in response to rising electricity consumption, diminishing fossil fuel reserves in addition to the need for reducing carbon emissions. Among the available sources of renewable energy, photovoltaic (PV) power generation is the most promising technology with enormous potential and easy access. This paper presents an optimum control technique for grid connected PV systems. The improved single ended primary inductor converter (SEPIC) controls and regulates PV output power to the optimum voltage level. The working of the improved SEPIC is controlled by a proportional-integral (PI) controller optimized by meta-heuristic technique of lion swarm optimization (LSO). The constant output from the converter is then supplied to the power grid through a single-phase voltage source inverter (1 ϕ VSI). The effectiveness of the proposed control strategy is ascertained using hardware validation with DSPIC3050FPGA controller and MATLAB simulation generating a reduced total harmonic distortion (THD) of 3.9% and 2.9%, respectively. Furthermore, the proposed system generates an enhanced voltage gain of 1:10 and an efficiency of 96%.

This is an open access article under the [CC BY-SA](https://creativecommons.org/licenses/by-sa/4.0/) license.



Corresponding Author:

P. Annapandi

Department of Electrical and Electronics Engineering, Francis Xavier Engineering College

Tirunelveli, Tamil Nadu, India

Email: annapandian2001@gmail.com

1. INTRODUCTION

In recent days, the energy crisis is considered as a rising problem due to its influence on economic growth of all sectors [1]. Moreover, the fossil fuel burning results in greenhouse gas emission and global warming leading to environmental pollution. All these factors paved for the need of renewable energy resources (RESs) [2]. The photovoltaic (PV) systems are regarded as significant clean and popular renewable energy resource and is applied for both grid integration and power generation. The factors related to PV system including grid integration, efficiency, grid stability, and quality of uninterrupted power are a serious concern. Hence, the improvement of PV system efficiency and reduction of installation costs are focused by Rodriguez *et al.* [3].

Generally, dozens of PV panels are used for improving the voltage at the terminals [4]. The number of PV panels adopted for a particular application is reduced with the use of converter [5]. It is an important component used for a removal of the power from the photovoltaic array and it maintains low current

ripples [6], [7]. Added to improved efficiency and reduced cost, the DC-DC converters provide fast current and voltage control along with wide range of input/output voltage change ratios [8]. The conventional converters are boost and buck-boost converters that perform enlarging of input voltage range obtained from the PV array [9]. However, achieving conversion gain beyond six practically is not feasible in these converters. The increased duty cycle operation compromises an efficiency of boost converter but generate current ripples and electromagnetic interference [10]. Conventional Cuk converters have reduced switching losses, better efficiency, and superior voltage moderation, yet they showed restrictions in delivering sharp speed up/down voltage [11]. The single ended primary inductor converter (SEPIC) is used in various applications related to power electronics due to its unique properties and many works concentrate on improving its step-up voltage gain. The possibility of soft-switching performance without the addition of auxiliary elements is a unique feature of SEPIC [12]–[14]. Generally, an increased voltage gain is attained in SEPIC by coupled inductor as well as isolated transformer approaches. These approaches in turn exhibit the drawbacks of isolated and coupled inductors whereas converters with non-coupled inductor have reduced voltage gain [15]. Considering the aforementioned shortcomings, the SEPIC requires further improvement to enhance its performance and generate improved voltage gain ratio.

In order to sustain a constant DC link voltage, a closed loop control is preferred which employs proportional-integral (PI) controller. It is the most feasible and simplest controller used for wide operating conditions [16]. The settling time requirement is satisfied by the proportional gain and steady state error is decreased by an integral gain. The PI controllers track the reference values and hence a satisfactory steady and dynamic response is determined by the fine-tuning of PI controller [17]. Considering uncertain, non-linear and complex systems, tuning of PI controller parameters is challenging with the adopting of traditional approaches like linear programming [18]. Initially, trial and error, conventional Ziegler-Nichols approaches are utilized for the tuning of polarization index controller parameters but they are not appropriate for random load variations [19]. The optimization approaches are alternate methods for tuning PI controllers in which the PI gains are estimated by these approaches [20]. The selection of the PI controller parameters is crucial and recently, several nature inspired algorithms are employed for the optimization process [21], [22]. The power obtained from DC link is distributed to the grid by means of a voltage source inverter which injects an AC output to grid with reduced total harmonic distortion (THD) [23]. Due to grid disturbances and voltage distortion at point of common coupling (PCC) by nonlinear loads, grid synchronization is considered as a challenging task [24]. The significant focus of grid synchronization is to enhance the control performance thereby injecting a high-quality power in the grid [25].

Therefore, the contributions of this research are concluded as below: An efficient grid-connected PV system is designed with improved SEPIC for boosting the input power from PV array. A novel lion swarm optimization is proposed for the tuning of PI controller parameters which in turn effectively controls the converter operation for maintaining a constant DC link voltage. The obtained power with reduced harmonics is fed to a grid through a 1ϕ VSI for providing effective grid synchronization by delivering appropriate reactive power.

2. PROPOSED SYSTEM DESCRIPTION

The PV systems show a remarkable progress from a basic standalone site to large grid connected systems. The interconnection of PV with the grid aids in ensuring ceaseless supply of power. The need for control and supervision algorithms increases due to the wide adopting of PV systems worldwide. Here an efficient optimization algorithm for grid connected PV using improved SEPIC is adopted as presented in Figure 1.

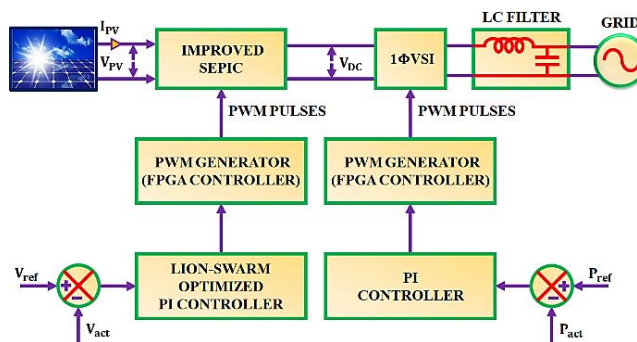


Figure 1. Block diagram of the proposed work

The obtained solar power from photovoltaic system relies on the intensity and illumination of the light which necessitates the usage of a converter. Hence, improved SEPIC is employed to improve the lower photovoltaic output voltage and also buck the output voltage at times of huge intensity. A constant output is maintained at the DC link by a PI controller which adopts lion swarm optimization for tuning its gain parameters. The algorithm provides superior results with improved convergence speed and robustness thereby generating enhanced proportional and integral gains. The DC voltage is further supplied to grid through a 1ϕ VSI with LC filter which in turn provides effective synchronization and reduced THD with the help of conventional polarization index controller. A whole setup provides a stable power supply to the grid in an effective manner.

2.1. PV system

In case of a PV connected to grid, the generated power is uploaded to grid for the process of direct transmission, distribution and consumption. Generally, operating temperature and irradiance of the PV cell influence an output characteristic of a photovoltaic. Figure 2 depicts the PV system's equivalent circuit.

The equations for current and voltage are given by (1) and (2).

$$I_{ph} = I_D + I + \left(\frac{V_D}{R_{sh}}\right) \tag{1}$$

$$V = V_D - (I * R_s) \tag{2}$$

Here, the diode current I_D is given by (3).

$$I_D = I + \left(e^{(V_D/V_T)} - 1\right) \tag{3}$$

The characteristics of voltage and current which aids in the analysis of irradiance variation and temperature effect is predict in (1) and (2). When the irradiance shows variations, the fluctuations of open circuit voltage is small whereas short circuit current exhibits sharp fluctuations. These factors affect the output voltage of photovoltaic system and this demands the adopting of an efficient DC-DC converter for enhancing the photovoltaic output.

2.2. Improved SEPIC operation

The output obtained from PV system is not sufficient for the grid operation and this obtains the need of a DC-DC converter. Among them, SEPIC is known for its improved voltage gain but can be further improved to meet the standard of high static gain. Hence an improved SEPIC is proposed in this work which accomplishes the addition of a diode D_1 , a capacitor C_1 as represented in Figure 3. The output voltage reversing the polarity of the capacitor C_s charges the capacitor C_1 . The improved SEPIC performs its operation in continuous conduction mode (CCM) and the different modes of operation are explained below.

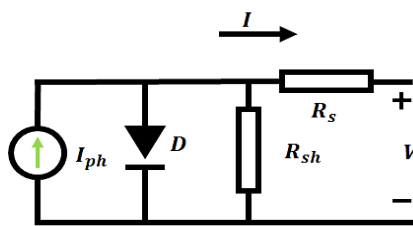


Figure 2. Photovoltaic system

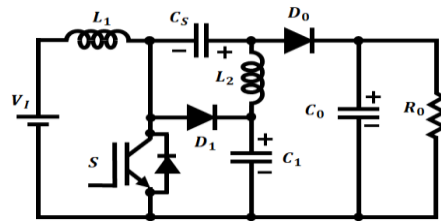


Figure 3. Improved SEPIC

2.2.1. Mode 1

The mode 1 operation of improved SEPIC in which switch S is turned off at time t_0 as represent in Figure 4. An input inductor L_1 transfers stored energy to the output side through diode D_0 and capacitor C_s . Moreover, the stored energy of L_1 is moved to a capacitor C_1 through the diode D_1 . Similarly, the inductor L_2 transfers the stored energy to the output through a diode D_0 .

2.2.2. Mode 2

In Figure 5 the equivalent circuit of mode 2 operation in which switch S is turned on at time t_1 is represented. The diodes D_0 and D_1 are blocked in this mode and the inductors L_1, L_2 continues to store energy. The inductor L_1 gets supplied with the input voltage and the inductor L_2 gets supplied with V_{C_s} and V_{C_1} in which V_{C_1} is greater than V_{C_s} . A voltage across C_1 is similar to the maximum voltage across all diodes

and the switch. The total voltage across the capacitors C_1 and C_s indicate the output of a converter. The average current of an inductor L_1 and average current of an inductor L_2 are equivalent to the input current and output current respectively. During steady state condition, an average voltage over inductor is zero.

$$\frac{T_{on}}{T_{off}} = \frac{(V_{c1}-V_I)}{V_I} \tag{4}$$

Consider,

$$\alpha = \frac{T_{on}}{T_{off}} \tag{5}$$

where, α indicates the duty cycle, T_{on} represents the on time, T_{off} represents the off time. The relation between voltage across the capacitor V_{cs} and input voltage V_I is given by (6).

$$\frac{V_{c1}}{V_I} = \frac{1}{(1-\alpha)} \tag{6}$$

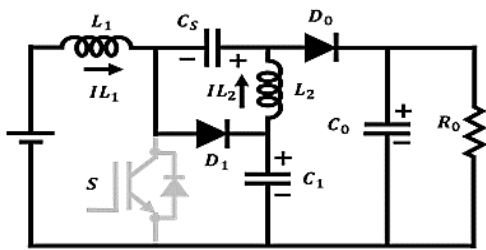


Figure 4. Mode 1 operation

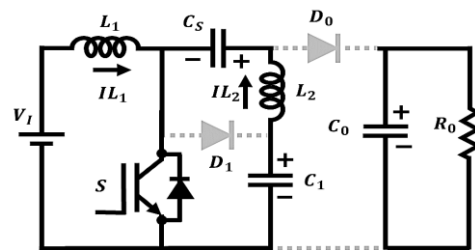


Figure 5. Mode 2 operation

At turned-off condition of the switch S , the diodes D_0 and D_1 are in on state, the output voltage V_0 is mentioned as (7).

$$V_0 = V_{c1} + V_{cs} \tag{7}$$

The voltage across the capacitor V_{cs} is given by (8).

$$V_{cs} = V_0 - V_{c1} \tag{8}$$

Substitute (6) and (8) in (7) we get (9).

$$\frac{V_0}{V_I} = \frac{(1-\alpha)}{(1+\alpha)} \tag{9}$$

The gain of the improved SEPIC which clearly indicates that the output gain highly relies on duty cycle value is represents in (9). The obtained output DC voltage from converter is further fed to DC link at which a constant voltage has to be maintained. In order to accomplish this, a closed loop control based on PI controller is needed, as explained below.

2.3. Lion swarm optimized PI controller

Generally, DC link voltage has to be maintained at a constant level for achieving satisfactory results without fluctuations. This is achieved by a PI controller which processes the error value obtained by the comparison of the reference voltage and an actual DC link voltage. An error value applied to the PI controller has to be zero which is attained by appropriate values of K_p and K_i parameters. This tuning of PI parameters is done by optimization approaches and this work proposes lion swarm optimization for finding values of K_p and K_i parameters.

2.3.1. Lion swarm optimization

The lion is regarded as most social exhibiting improved levels of antagonism and cooperation. They are classified as lion cubs, lioness and lion king where the dominance is high in lion king, since it is required to remain stronger to retain its dominant position. The hunting lions are the lionesses, which breeds the lion cubs, recognizes the prey location and encircles them while approaching the prey. The term following lions is

associated to the lion cubs and are protected by the lion king. Lion cubs are taught about hunting by the lioness and they seek lion king for food at times of hunger. Considering the swarm, the lions coordinate among themselves as a team for searching food. The optimization algorithm shown in Figure 6 relies on the hunting behavior of the swarm and the lion king is the one with best fitness value. On identifying a prey, the lion king moves towards the prey's position whereas the lion cubs follow the lioness for learning the hunting process.

The adult lion's proportional factor is given by β which is a random positive number within [0,1] range and in this work β is set as 0.5. The term α_f is used to represent the disturbance factor in moving range of the lioness, which enhances the convergence speed by balancing the global exploration as well as local exploitation. It is given by (10).

$$\alpha_f = step_1 \cdot \exp\left[-30 \cdot \frac{t}{T}\right]^{10} \quad (10)$$

Here, T - maximum iteration, t - current iteration, value of step within lionesses' range of activity $step_1$ is provided as (11).

$$step_1 = \alpha_1 \cdot (\bar{x}_{max} - \bar{x}_{min}) \quad (11)$$

Here, for every dimension, the maximal and minimal mean value is represented by \bar{x}_{max} and \bar{x}_{min} respectively, α_1 denotes the control factor. The lion cubs' moving range disturbance factor is denoted by the symbol α_c and is determined by (12).

$$\alpha_c = step_2 \cdot \frac{T-t}{T} \quad (12)$$

Where,

$$step_2 = \alpha_2 \cdot (\bar{x}_{max} - \bar{x}_{min}) \quad (13)$$

Here, α_2 denotes the control factor and is any number within the scale [0,1]. The position of all lions is denoted by (14).

$$x = \begin{bmatrix} x_{1,1} & x_{1,2} & \dots & x_{1,D} \\ \vdots & \vdots & & \vdots \\ x_{n,1} & x_{n,2} & \dots & x_{n,D} \end{bmatrix} \quad (14)$$

Here $x_{i,j}$ denotes j^{th} dimension related to i^{th} lion, each D dimensional vector $x_i = (x_{i,1}, x_{i,2}, \dots, x_{i,D})$ denote the state of i^{th} lion and is provided by (15).

$$x_{i,j} = x_{min,j} + rand(0,1) \cdot (x_{max,j} - x_{min,j}) \quad (15)$$

Here, $i = 1, 2, \dots, n$ and $j = 1, 2, \dots, D$, $rand(0,1)$ specifies a random number which is uniformly distributed in range [0,1], $x_{max,j}$ denotes upper bound and $x_{min,j}$ denotes lower bound of j^{th} dimension. The number of the adult lions is given as below.

$$nLeader = [n \cdot \beta] \quad (16)$$

And the number of lion cubs is given by $n - nLeader$ the appropriate fitness values are below.

$$f = \begin{bmatrix} f_1([x_{1,1}, x_{1,2}, L, x_{1,D}]) \\ f_2([x_{2,1}, x_{2,2}, L, x_{2,D}]) \\ \vdots \\ f_n([x_{n,1}, x_{n,2}, L, x_{n,D}]) \end{bmatrix} \quad (17)$$

Quality of prey sought by each lion is represented by the fitness value of its position. As a result, their chances of survival are likewise increased. Each lion's place in lion swarm optimization (LSO) is modified based on its own experience as well as that of its neighbors. As previously stated, the hunting mechanisms of each lion is different during the hunting phase. Around the prey, a circle shaped neighborhood is created in order to support lions coming from various directions, thus the problem of trapping in local optima is successfully avoided. The increase in population diversity is also possible using this scheme.

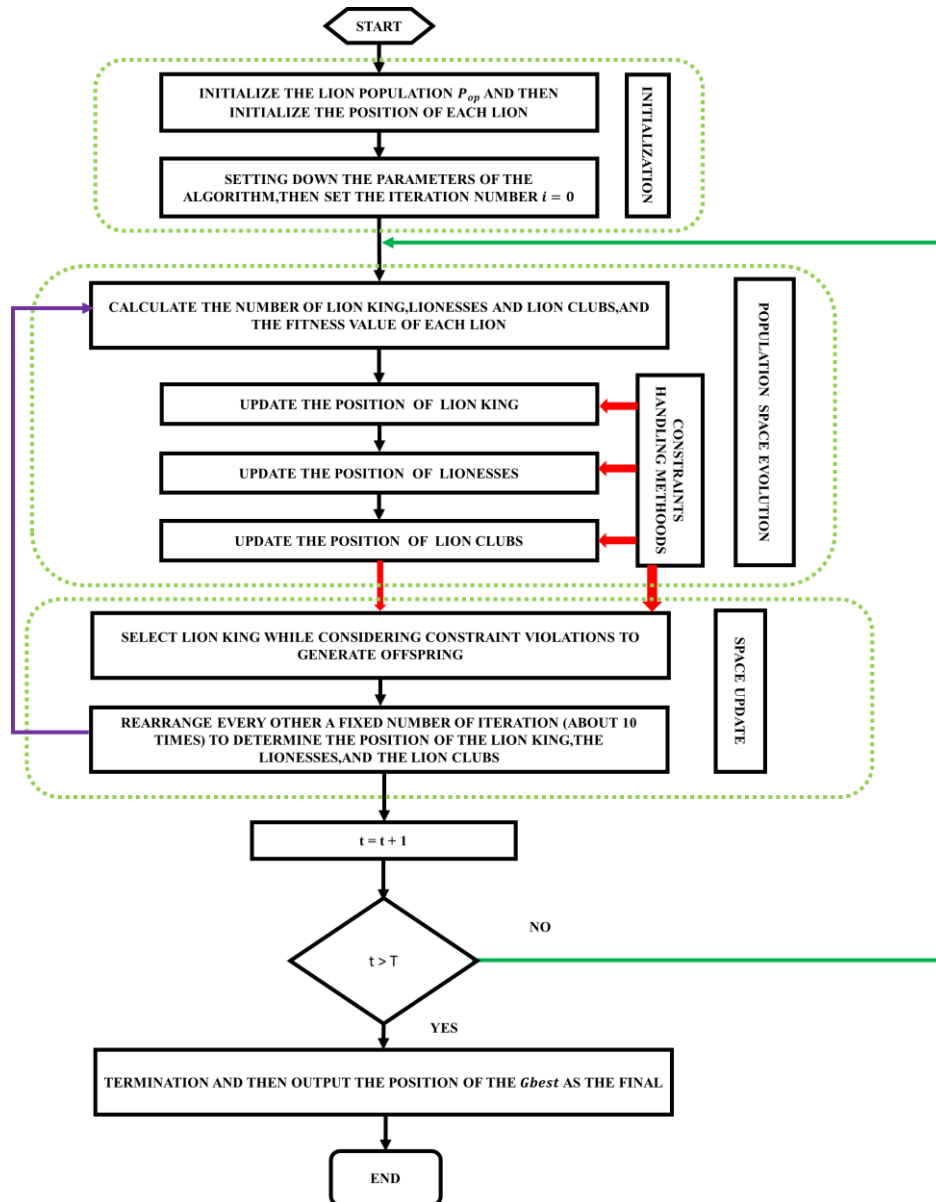


Figure 6. Flow chart of lion swarm optimization

The position with the least fitness value is the destination of the lion king, to increase that he has priority for catch over the other lions. New status of lion king, as in (18).

$$x_i(t+1) = gbest(t) \cdot (1 + \gamma \cdot \|pbest_i(t) - gbest(t)\|) \quad (18)$$

Where, t = present iteration value, $gbest(t)$ = at t , the globally best position of catch, γ = random number lies between $[0, 1]$ $pbest_i(t)$ = at t , best position of i^{th} lion.

Lionesses often hunt by recognizing their prey's position, encircling them, and then attacking them. When a lioness engages in hunting behavior, she usually does so with the help of another lioness. The collaboration lioness is the lioness who was chosen from the lioness group by someone other than herself.

How the new lioness position might be obtained in this case is shown in (19).

$$x_i(t+1) = \frac{pbest_i(t) + pbest_c(t)}{2} \cdot (1 + \alpha_f \cdot \gamma) \quad (19)$$

Where, α_f -, moving range disturbance factor of lioness. $pbest_c(t)$ -, at t , cooperation lioness best position. The new position of lion cub is given by (20).

$$x_i(t + 1) = \begin{cases} \frac{gbest(t)+pbest_i(t)}{2} \cdot (1 + \alpha_c \cdot \gamma), & q \leq \frac{1}{3} \\ \frac{pbest_m(t)+pbest_i(t)}{2} \cdot (1 + \alpha_c \cdot \gamma), & \frac{1}{3} < q < \frac{2}{3} \\ \frac{\overline{gbest}(t)+pbest_i(t)}{2} \cdot (1 + \alpha_c \cdot \gamma), & \frac{2}{3} \leq q \leq 1 \end{cases} \quad (20)$$

Where, $pbest_m(t)$ –best position followed by lion cub, as in (21).

$$\begin{aligned} &\overline{gbest}(t) - \text{Position of } i^{th} \text{ lion cub} \\ \overline{gbest}(t) &= \overline{x_{max}} + \overline{x_{min}} - gbest(t) \end{aligned} \quad (21)$$

α_c – moving range disturbance factor, q -random number range [0, 1]. Based on the values of $gbest$ and $pbest$, optimal outputs are obtained which are used for the efficient tuning of the K_p and K_i parameters. The obtained values of PI controller parameters outperform the existing methods which in turn efficiently controls the operation of improved SEPIC for maintaining a constant DC link voltage.

2.4. Grid connected 1ϕ VSI

Generally, the low powered PV systems are connected to AC grid through 1ϕ inverters. Voltage source inverter executes active mitigation of harmonics with the implementation of an LC filter as well as the associated circuit diagram is represented in Figure 7. A conventional PI controller achieves grid synchronization by reducing the error between the real and reference power values. The outputs obtained are converted to appropriate pulses to be fed to VSI. Voltage source inverter changes the DC voltage from the DC link into AC form for grid injection. The Voltage source inverter operates as a current source rather than a voltage source while in grid linked mode. An inverter injects higher quality power into the grid at controllable changes in voltage, frequency, and phase angle as a consequence of the synchronization. On the single-phase grid, this outcomes in the output being a high-quality integrated voltage. Thus, a proposed methodology effectively presents a grid connected PV system with improved SEPIC adopting lion swarm optimized PI controller for the production of improved outputs.

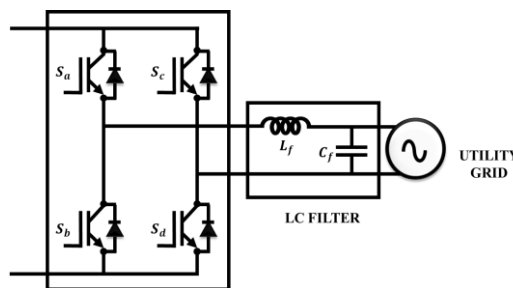


Figure 7. 1ϕ grid connected VSI

3. RESULTS AND DISCUSSION

The grid connected PV systems contribute to majority of the installed capacity worldwide when compared to battery utilized standalone systems. These systems adopt an efficient converter along with control approaches for maintaining a constant DC link voltage. This work proposes an improved SEPIC with lion swarm optimization and the corresponding simulation is performed in MATLAB/Simulink. Table 1 gives the specifications of solar panel as well as improved SEPIC converter.

Table 1. Design parameter specifications

Parameter	Values	Parameter	Values
Power	2000 W	Input capacitor C_1, C_s	870 μF
No of solar panels connected in series	36	Output capacitor C_o	2200 μF
No of panels	100 W, 20 panels	Switching frequency f_s	10 kHz
L_1, L_2	5 mH	R_o	100 Ω

Initially, the input solar irradiance is maintained at 980 W/m² for 0.1s and then it is increased to 1000 W/m² as indicated in Figure 8(a). The solar irradiance is varied to evaluate the dynamic nature of the

suggested control technique in non-linear operating conditions. In accordance to the increase in irradiance, the PV voltage also increases from 79 V to 80 V at 0.1 sec as depicted in Figure 8(b).

Figures 9(a) and 9(b) specifies an input current and output power waveform of a PV panel. As demonstrated by Figure 9(a), the photo generated current from the PV is 17.2 A till 0.1s and it increases to 18.8 A corresponding to the change in irradiance. Similar to this, Figure 9(b) shows that the PV power which is initially 1360 W, becomes 1500 W at 0.1s in response to the increase in irradiance.

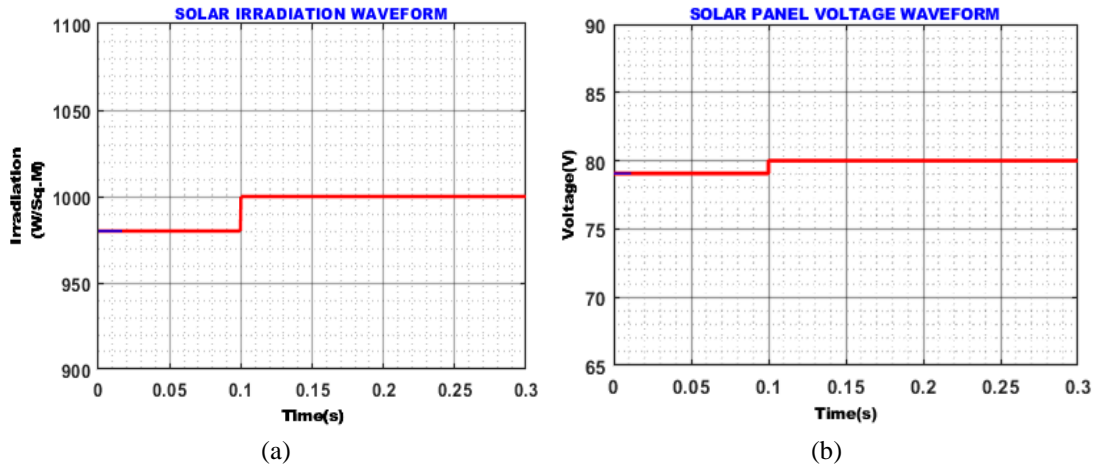


Figure 8. PV parameter waveform: (a) irradiation and (b) voltage

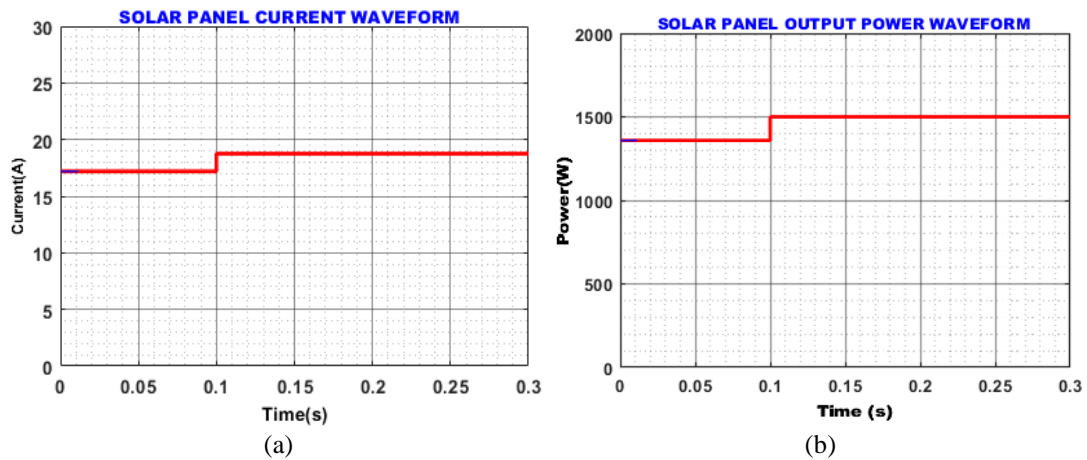


Figure 9. Waveforms of PV: (a) input current and (b) output power

The output of the improved SEPIC for different control techniques is illustrated in Figure 10. The converter output with the employment of PI controller seen in Figure 10(a) is affected by peak overshoot condition at first and then it delivers a voltage of 270 V from 0.12 s. However, the output that is obtained is unstable and is affected by fluctuations. Figure 10(b) illustrates GWO based PI controller output, where peak overshoot condition arises as like PI controller, but it is able to provide a stable voltage at a quicker time of 0.1 s. Finally, the proposed lion swarm optimized PI is successful in providing an output without peak overshoot condition in quickest settling time of 0.08s, which is evident from Figure 10(c). Moreover, the change in operating conditions does not have an impact on the output of the lion swarm optimized PI based improved SEPIC. A stable voltage and current of 230 V, 5 A is obtained from the single-phase grid as shown in Figure 11. Additionally, as Figure 12 indicates, the suggested control approach is successful in minimizing THD at 2.9%.

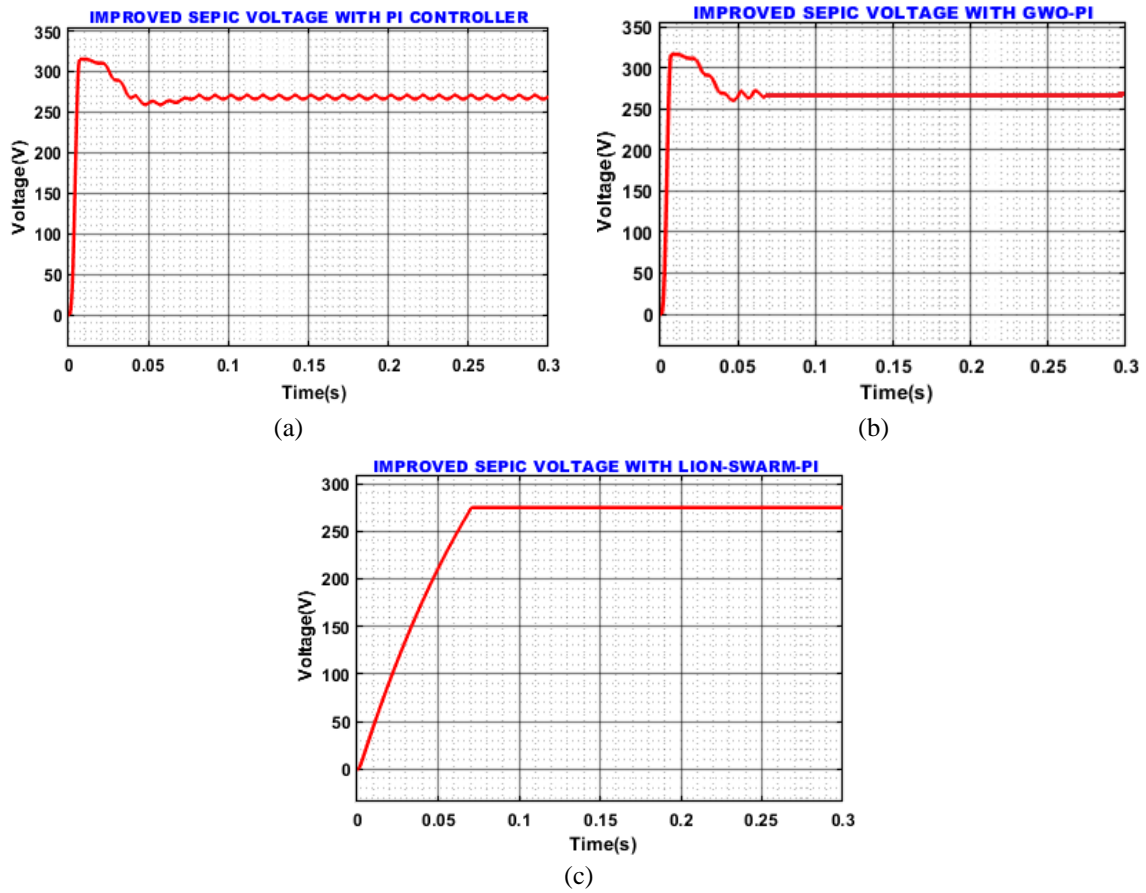


Figure 10. Output voltage of improved SEPIC: (a) with PI controller, (b) GWO-PI, and (c) lion swarm-PI

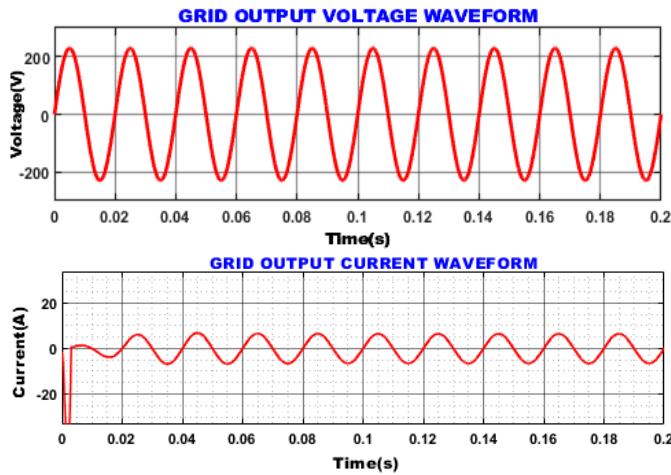


Figure 11. Grid output voltage and current

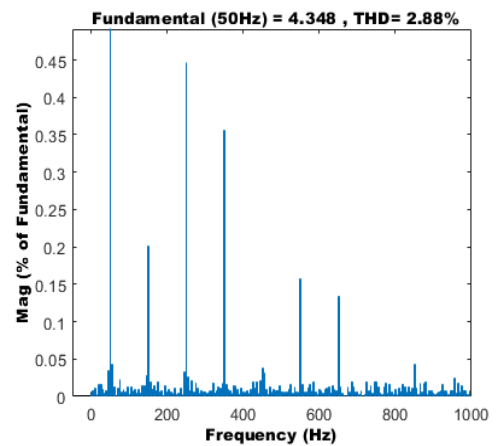


Figure 12. THD output

3.1. Hardware results

The proposed concept is experimentally validated using field programmable gate arrays (FPGA), and the properties of the introduced power conversion system are examined. FPGAs are a great alternative because of qualities like great configurability and performance. To implement the hybrid system in FPGA, the entire module has to be converted to an FPGA synthesizable module and the hardware implementation is carried out in DSPIC3050FPGA controller as shown in Figure 13.

The hardware validation of the proposed work generates the following outputs which indicates the efficacy of the proposed system. The corresponding waveforms are presented below with a detailed analysis. The input solar irradiance is presented in Figure 14, where a slight increase in value of solar irradiance is seen at one point. This definitely influences the operation of PV panel which in turn generates varying outputs.

Figure 15 demonstrates a photovoltaic panel current waveform and output voltage, which highly relies on available temperature, solar irradiation and other environmental conditions. So, a variation in voltage output with the change in solar irradiation is observed from the waveform, seen in Figure 15(a). Similar to the PV voltage output, Figure 15(b) depicts the output current also increases in line with the rise in solar irradiation. As seen in Figure 16, the improved SEPIC converter produces a stable, controlled output with less amount of ripple contents. By boosting efficiency and decreasing input current ripples, the improved SEPIC solves the shortcomings of regular SEPIC.



Figure 13. Hardware setup

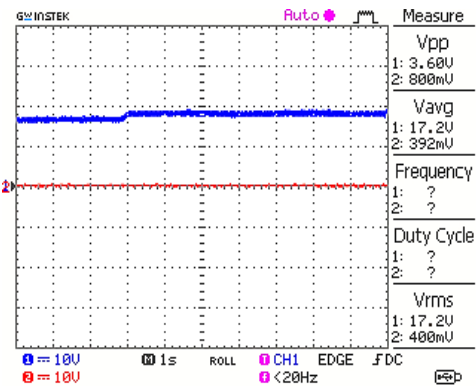
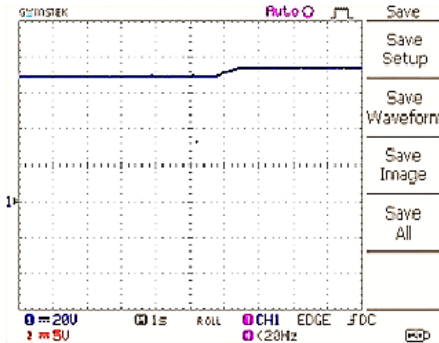
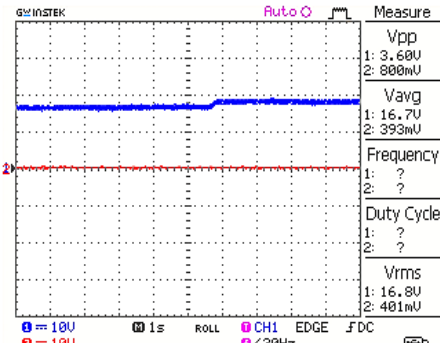


Figure 14. Solar irradiation



(a)



(b)

Figure 15. Photovoltaic panel: (a) output voltage and (b) output current

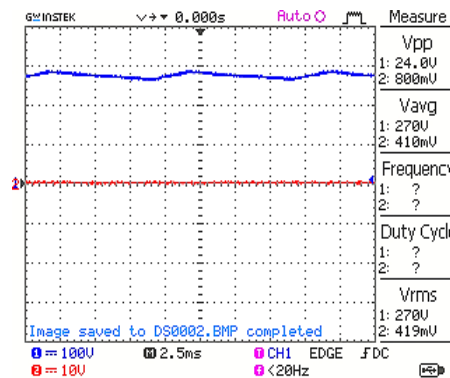


Figure 16. Output voltage of improved SEPIC

Figures 17(a) and 17(b) show a timeline of the voltage and current variations on the grid. These graphs provide information about the dynamic voltage and current behaviour inside the grid system. This indicates an enhanced grid synchronization by the proposed topology.

The THD value is to be kept as low as possible for the system's stability and improved power quality. The implementation of the proposed approach yields a lower THD value, and Figure 18 illustrates the corresponding output. Figure 19(a) displays the efficacy comparison between improved SEPIC and conventional converters such as buck-boost, Cuk, boost, and SEPIC. From figure it is observed that improved SEPIC has a better efficiency of 96% respectively. The improved SEPIC converter's performance is then displayed in Figure 19(b), where the voltage gain value is 1:10, which is relatively higher than state of art converter topologies.

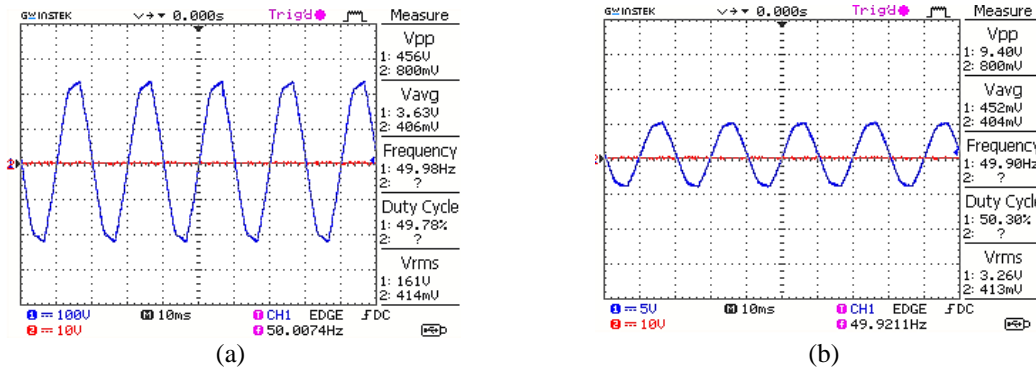


Figure 17. Grid: (a) voltage and (b) current

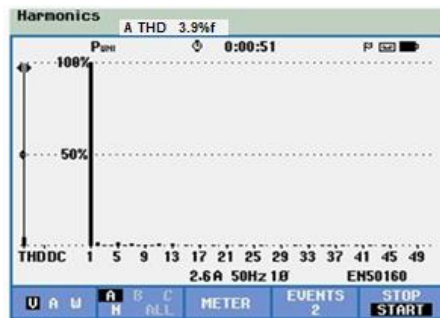


Figure 18. THD output

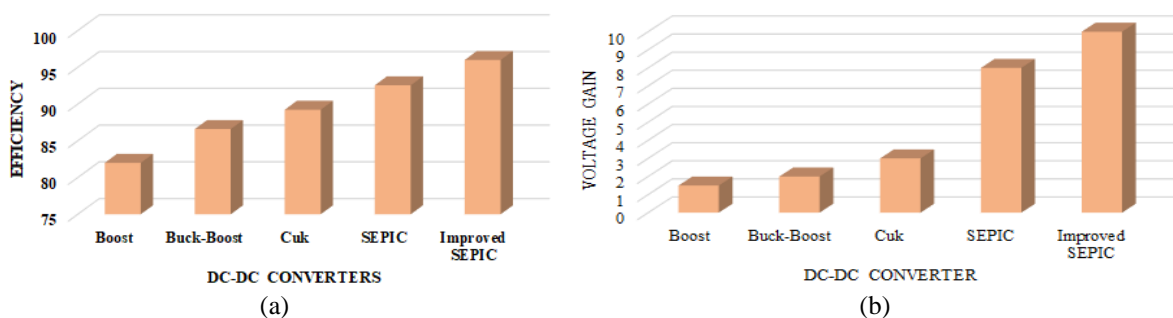


Figure 19. DC-DC converter: (a) efficiency comparison and (b) voltage gain comparison

The obtained THD values for current are compared with Cuk and SEPIC as shown in Figure 20(a). The proposed converter generates an improved THD of 2.9% and 3.9% for simulation and hardware implementation respectively. The settling time of lion swarm optimized PI controller is contrasted with conventional PI controller and GWO based PI controller in Figure 20(b). From given comparison chart, it is determined the proposed control technique offers the fastest settling time of 0.08s in case of simulation and 0.09s in case of hardware validation.

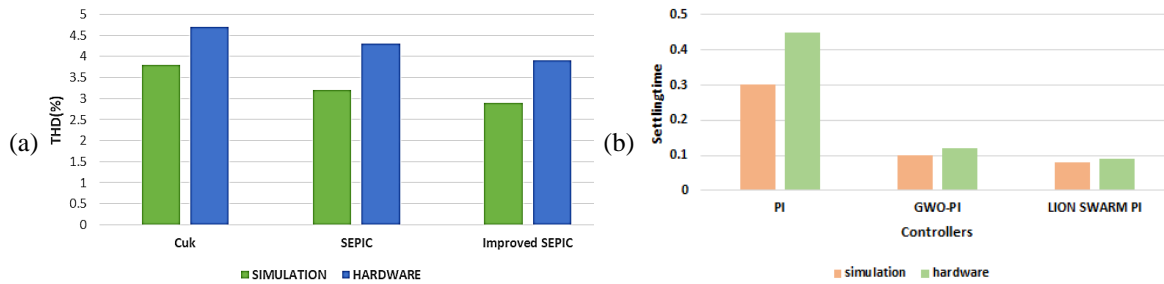


Figure 20. Performance measure of (a) current THD and (b) settling time of controllers

4. CONCLUSION

An optimum control strategy for grid connected photovoltaic systems is presented in this study, since grid-connected PV systems account for the vast majority of installed capacity worldwide when compared to battery-based standalone systems. The voltage derived from the photovoltaic panel is transformed to the desired level using improved SEPIC of high voltage gain and an efficiency of 96%. The improvement of dynamic performance indices of converter in terms of over shoot and settling time is achieved using lion swarm optimized PI controller. Thus, from the obtained outcomes, it is noted that the suggested control technique is successful in eliminating the overshoot problem in the converter and provides a quick settling time of 0.08s for simulation and 0.09s for hardware validation.

REFERENCES

- [1] K. S. Kavin and P. S. Karuvelam, "PV-based grid interactive PMBLDC electric vehicle with high gain interleaved DC-DC SEPIC converter," *IETE Journal of Research*, vol. 69, no. 7, pp. 4791–4805, Sep. 2023, doi: 10.1080/03772063.2021.1958070.
- [2] A. Kumar and P. Kumar, "Power quality improvement for grid-connected PV system based on distribution static compensator with fuzzy logic controller and UVT/ADALINE-based least mean square controller," *Journal of Modern Power Systems and Clean Energy*, vol. 9, no. 6, pp. 1289–1299, 2021, doi: 10.35833/MPCE.2021.000285.
- [3] P. Rodriguez, C. Citro, J. I. Candela, J. Rocabert, and A. Luna, "Flexible grid connection and islanding of SPC-based PV power converters," *IEEE Transactions on Industry Applications*, vol. 54, no. 3, pp. 2690–2702, May 2018, doi: 10.1109/TIA.2018.2800683.
- [4] F. Rong, X. Gong, and S. Huang, "A novel grid-connected PV system based on MMC to get the maximum power under partial shading conditions," *IEEE Transactions on Power Electronics*, vol. 32, no. 6, pp. 4320–4333, Jun. 2017, doi: 10.1109/TPEL.2016.2594078.
- [5] M. I. Marei, B. N. Alajimi, I. Abdelsalam, and N. A. Ahmed, "An integrated topology of three-port DC-DC converter for PV-battery power systems," *IEEE Open Journal of the Industrial Electronics Society*, vol. 3, pp. 409–419, 2022, doi: 10.1109/OJIES.2022.3182977.
- [6] K. S. Tey, S. Mekhilef, M. Seyedmahmoudian, B. Horan, A. T. Oo, and A. Stojcevski, "Improved differential evolution-based MPPT algorithm using SEPIC for PV systems under partial shading conditions and load variation," *IEEE Transactions on Industrial Informatics*, vol. 14, no. 10, pp. 4322–4333, Oct. 2018, doi: 10.1109/TII.2018.2793210.
- [7] M. Forouzesh, Y. Shen, K. Yari, Y. P. Siwakoti, and F. Blaabjerg, "High-efficiency high step-up DC-DC converter with dual coupled inductors for grid-connected photovoltaic systems," *IEEE Transactions on Power Electronics*, vol. 33, no. 7, pp. 5967–5982, Jul. 2018, doi: 10.1109/TPEL.2017.2746750.
- [8] K. Nathan, S. Ghosh, Y. Siwakoti, and T. Long, "A new DC-DC converter for photovoltaic systems: coupled-inductors combined Cuk-SEPIC converter," *IEEE Transactions on Energy Conversion*, vol. 34, no. 1, pp. 191–201, Mar. 2019, doi: 10.1109/TEC.2018.2876454.
- [9] Q. Huang, A. Q. Huang, R. Yu, P. Liu, and W. Yu, "High-efficiency and high-density single-phase dual-mode cascaded buck-boost multilevel transformerless PV inverter with GaN AC switches," *IEEE Transactions on Power Electronics*, vol. 34, no. 8, pp. 7474–7488, Aug. 2019, doi: 10.1109/TPEL.2018.2878586.
- [10] Y. P. Siwakoti *et al.*, "High-voltage gain Quasi-SEPIC DC-DC converter," *IEEE Journal of Emerging and Selected Topics in Power Electronics*, vol. 7, no. 2, pp. 1243–1257, Jun. 2019, doi: 10.1109/JESTPE.2018.2859425.
- [11] S. Padmanaban, N. Priyadarshi, M. S. Bhaskar, J. B. Holm-Nielsen, E. Hossain, and F. Azam, "A hybrid photovoltaic-fuel cell for grid integration with Jaya-based maximum power point tracking: experimental performance evaluation," *IEEE Access*, vol. 7, pp. 82978–82990, 2019, doi: 10.1109/ACCESS.2019.2924264.
- [12] S. Hasanpour, M. Forouzesh, Y. Siwakoti, and F. Blaabjerg, "A new high-gain, high-efficiency SEPIC-based DC-DC converter for renewable energy applications," *IEEE Journal of Emerging and Selected Topics in Industrial Electronics*, vol. 2, no. 4, pp. 567–578, Oct. 2021, doi: 10.1109/JESTIE.2021.3074864.
- [13] D. S. Sankaralingam, M. S. B. Natarajan, M. Muthusamy, and S. B. Singh, "A novel metaheuristic approach for control of SEPIC converter in a standalone PV system," *International Journal of Power Electronics and Drive Systems (IJPEDS)*, vol. 13, no. 2, pp. 1082–1092, Jun. 2022, doi: 10.11591/ijpeds.v13.i2.pp1082-1092.
- [14] M. Vaigundamoorthi, R. Ramesh, V. V. Prabhu, and K. A. Kumar, "MPPT oscillations minimization in PV system by controlling non-linear dynamics in SEPIC DC-DC converter," *International Journal of Electrical and Computer Engineering (IJECE)*, vol. 10, no. 6, pp. 6268–6275, Dec. 2020, doi: 10.11591/ijece.v10i6.pp6268-6275.
- [15] S. A. Ansari and J. S. Moghani, "A novel high voltage gain noncoupled inductor SEPIC converter," *IEEE Transactions on Industrial Electronics*, vol. 66, no. 9, pp. 7099–7108, Sep. 2019, doi: 10.1109/TIE.2018.2878127.
- [16] M. S. Ali, L. Wang, H. Alquhayz, O. U. Rehman, and G. Chen, "Performance improvement of three-phase boost power factor correction rectifier through combined parameters optimization of proportional-integral and repetitive controller," *IEEE Access*, vol. 9, pp. 58893–58909, 2021, doi: 10.1109/ACCESS.2021.3073004.
- [17] S. Kakkar *et al.*, "Design and control of grid-connected PWM rectifiers by optimizing fractional order pi controller using water cycle algorithm," *IEEE Access*, vol. 9, pp. 125941–125954, 2021, doi: 10.1109/ACCESS.2021.3110431.

- [18] M. I. Mosaad, H. S. M. Ramadan, M. Aljohani, M. F. El-Naggar, and S. S. M. Ghoneim, "Near-optimal PI controllers of STATCOM for efficient hybrid renewable power system," *IEEE Access*, vol. 9, pp. 34119–34130, 2021, doi: 10.1109/ACCESS.2021.3058081.
- [19] V. Veerasamy *et al.*, "A hankel matrix based reduced order model for stability analysis of hybrid power system using PSO-GSA optimized cascade PI-PD controller for automatic load frequency control," *IEEE Access*, vol. 8, pp. 71422–71446, 2020, doi: 10.1109/ACCESS.2020.2987387.
- [20] T. Appala Naidu, S. R. Arya, R. Maurya, and S. Padmanaban, "Performance of DVR using optimized PI controller based gradient adaptive variable step lms control algorithm," *IEEE Journal of Emerging and Selected Topics in Industrial Electronics*, vol. 2, no. 2, pp. 155–163, Apr. 2021, doi: 10.1109/JESTIE.2021.3051553.
- [21] A. Ahmad *et al.*, "Controller parameters optimization for multi-terminal DC power system using ant colony optimization," *IEEE Access*, vol. 9, pp. 59910–59919, 2021, doi: 10.1109/ACCESS.2021.3073491.
- [22] A. M. Hussien, R. A. Turky, H. M. Hasanien, and A. Al-Durra, "LMSRE-based adaptive PI controller for enhancing the performance of an autonomous operation of microgrids," *IEEE Access*, vol. 9, pp. 90577–90586, 2021, doi: 10.1109/ACCESS.2021.3091496.
- [23] B. Guo *et al.*, "A robust second-order sliding mode control for single-phase photovoltaic grid-connected voltage source inverter," *IEEE Access*, vol. 7, pp. 53202–53212, 2019, doi: 10.1109/ACCESS.2019.2912033.
- [24] S. Swain and B. Subudhi, "Grid synchronization of a PV system with power quality disturbances using unscented Kalman filtering," *IEEE Transactions on Sustainable Energy*, vol. 10, no. 3, pp. 1240–1247, Jul. 2019, doi: 10.1109/TSTE.2018.2864822.
- [25] S. Kewat and B. Singh, "Grid synchronization of WEC-PV-BES based distributed generation system using robust control strategy," *IEEE Transactions on Industry Applications*, vol. 56, no. 6, pp. 7088–7098, Nov. 2020, doi: 10.1109/TIA.2020.3021060.

BIOGRAPHIES OF AUTHORS



P. Annapandi    received the bachelor Degree in Electrical and Electronics Engineering from Government college of Engineering, Tirunelveli Tamil Nadu in May 2000 and Master degree in power Electronics and Drives from College of Engineering, Guindy, Anna University, Chennai, Tamil Nadu, in May 2006, and Ph.D. in Electrical Engineering at Anna University, Chennai, Tamil Nadu, in 2013. His research interests include smart grid and power quality. He can be contacted at email: annapandian2001@gmail.com.



D. Lakshmi    associate professor of Department of Electrical and Electronics Engineering, Academy of Maritime Education and Training, deemed to be University, Chennai, Tamil Nādu, India. She has more than 22 years of expertise in the field of power system. She has guided more than 30 UG students, 15 PG students and 4 research scholars. She has published 6 book chapters and 4 books, 41 articles in SCI and Scopus indexed journals and nearly 25 national level and international level conferences proceedings. She has received many awards from various organizations for her contribution towards the assigned work. She is a life member in professional bodies such as IEEE, IEI, IAENG, and InSc. She is acting as editorial manager and reviewer for various reputed journals. She received many funds from Govt agencies and reputed organizations for contributing the recent research and product developments. She is a star organizer in Igen Energathon-2023 Marathon, a new world record on longest conference. Her areas of interest are power system operation and control, soft computing renewable energy systems, microgrid, and electrical machines. She can be contacted at email: lakshmiee@gmail.com.



B. Kavya Santhoshi    is working as an assistant professor in the Department of Electrical and Electronics Engineering at Godavari Institute of Engineering and Technology (A), Rajahmundry, Andhra Pradesh, India. She graduated in Electrical and Electronics Engineering at Saveetha Engineering College (Anna University), Chennai, Tamil Nadu, India. She secured Master of Engineering in Power Electronics and Drives at Jeppiaar Engineering College (Anna University), Chennai, Tamil Nadu, India. She secured Ph.D. in Electrical Engineering at Anna University, Chennai, Tamil Nadu, India. She is in the field of Power Electronics at Godavari Institute of Engineering and Technology (A), Rajahmundry, Andhra Pradesh, India. She is in teaching profession for more than 8 years. She has presented 30+ papers in National and International Journals, Conference, and Symposiums. Her main area of interest includes power electronics and renewable energy systems. She can be contacted at email: kavyabe2010@gmail.com.



P. Annapoorani    obtained Bachelor's degree in Electrical and Masters in Process Control and Automation. She has been teaching history for over 9 years. Presently working at Vel Tech Multi Tech Dr. Rangarajan Dr. Sakunthala Engineering College. Her area of interest in control systems, power systems. The area of interest includes control instrumentation and measurements. She contributed many numbers of active publications in reputed journals. She can be contacted at email: annapoorani@veltechmultitech.org.